AN ASSESSMENT OF CLEANING MECHANISMS DRIVEN BY POWER ULTRASOUND USING ELECTROCHEMISTRY AND HIGH-SPEED IMAGING TECHNIQUES

DOUGLAS OFFIN[A], CHRISTOPHER VIAN[A], PETER BIRKIN[A], TIMOTHY LEIGHTON[B]

[A]School of Chemistry
[B]ISVR
University of Southampton
Highfield, Southampton, SO17 1BJ, UK
prb2@soton.ac.uk

The cleaning of a surface is monitored in real time using a number of physical measurements. In particular an electrochemically inactive material is removed from an electrode while the electrode is able to detect a redox system in the bulk liquid. The removal of the material from the surface is monitored as an increased Faradaic current at the electrode surface. This signal is used to assess the ability of the cleaning method employed, in this case the application of power ultrasound to the system, as a function of the position of the electrode with respect to the sound source. It is shown that, depending on the conditions employed, surface cleaning is driven by different mechanisms. In order to validate these findings high-speed imaging of the system was undertaken and the results correlated with the electrochemical data. In addition a number of novel electrodes were also employed to assess the cleaning efficiency as a function of the electrode geometry employed. Implications for surface cleaning in the presence of power ultrasound are suggested.

INTRODUCTION

The cleaning of a surface using power ultrasound is a ubiquitous tool available in many laboratories. In many instances samples are either cleaned prior to further processing or dispersed within a suitable media as part of a larger methodology. In many instances cleaning or processing is facilitated by the employment of ultrasonic baths. This invariably involves the emersion of a suitable container within the bath. However, other ultrasonic sources are available. These include cylindrical reactors and ultrasonic probes or horns. In each case the sound field generated by these systems is different and will be affected by the geometry of the material, the materials acoustic properties, the bubble population, the ultrasonic field

generated by the source, the liquid properties and the geometry of the vessel [1-5]. Hence reproducibility between experiments and labs is difficult to achieve without careful consideration of the experimental protocol employed in each experiment. However, the cleaning action is often attributed to the generation of cavitation within the vessel itself and the interaction of these phenomena with the walls of the object in question. This interaction may take the form of jetting, microstreaming, shock impingement on the surface or the generation of chemical species with the ability to clean the material in question. Unsurprisingly the exact mechanism is often associated with 'transient cavitation' or more precisely inertial cavitation [5-7] where the violent collapse phase results in the local generation of these extreme conditions. Here the collapse phase of the bubble process is dominated by the converging inertia of the liquid rather than the pressure within the gas phase (which, if dominant, results in non-inertial cavitation). It should be remembered that inertial collapse requires specific local conditions to be met. For example, the liquid, the initial bubble size and the pressure field at that point are all key components. Apfel *et al.* have developed a model which enables the prediction of the fate of a bubble over one pressure cycle. Here a threshold pressure can be obtained [5-10]. In this theory two basic criteria must be met before 'inertial cavitation' can be generated. First, the pressure amplitude (note a sinusoidal pressure field is assumed) must be greater than the Blake pressure (the pressure amplitude required to drive rapid expansion of the initial bubble in question) [5]. Second, the maximum bubble radius produced by the pressure cycle must be greater than ~ $2.3R_0$ (where R_0 is the initial bubble size). This second criteria was associated with the maximum possible temperature [11, 12] expected within the gas phase at bubble collapse. Under these conditions it is possible to predict those bubbles that can be termed inertial or non-inertial at one moment in time and under a set of specific conditions. However, the bubble population is a dynamic regime and hence bubble growth and dissolution will also influence the situation. Nevertheless, if the acoustic pressure amplitude is too low then all bubbles present will be termed non-inertial. In water this threshold can be calculated to be ~ 120 kPa at 23 kHz [13]. Hence if we attribute all cleaning action to the generation of inertial cavitation, then the system must be designed to produce bubbles close the solid/liquid interface of the object to be cleaned and then to drive them with an appropriate sound wave sufficient to produce inertial collapse. Clearly an interesting question is raised. Is it necessary for cleaning that inertial cavitation is generated? This manuscript attempts to assess some of the key components relevant to this question using an electroanalytical approach in combination with high-speed imaging of the system and an understanding of the acoustic field generated in the test vessel employed.

In order to assess the cleaning action of an ultrasonic source, electrochemical experiments are employed to quantify the effect of cavitation on the surface of a material. In these experiments, the erosion of material from a surface is monitored as a function of distance between the sound source and the electrode surface. Later, a set of experiments detailing surface cleaning (here defined as the removal of an inert material from the electrode surface) is reported.

The effect of power ultrasound on surfaces has been well documented [14-16]. Indeed the presence of cavitation generated by flow, sound or some other technique is well known to have a detrimental effect on a surface. However, this characteristic can be used to quantify the presence of erosive mechanisms in this environment. In order to achieve this, a passivated electrode surface can be deployed [13, 17, 18]. Typical examples of this include Pb coated with an electrochemically generated $PbSO_4$ film, a stainless steel electrode and an aluminium electrode. In all these cases it is possible to use electrochemical control of the surface to

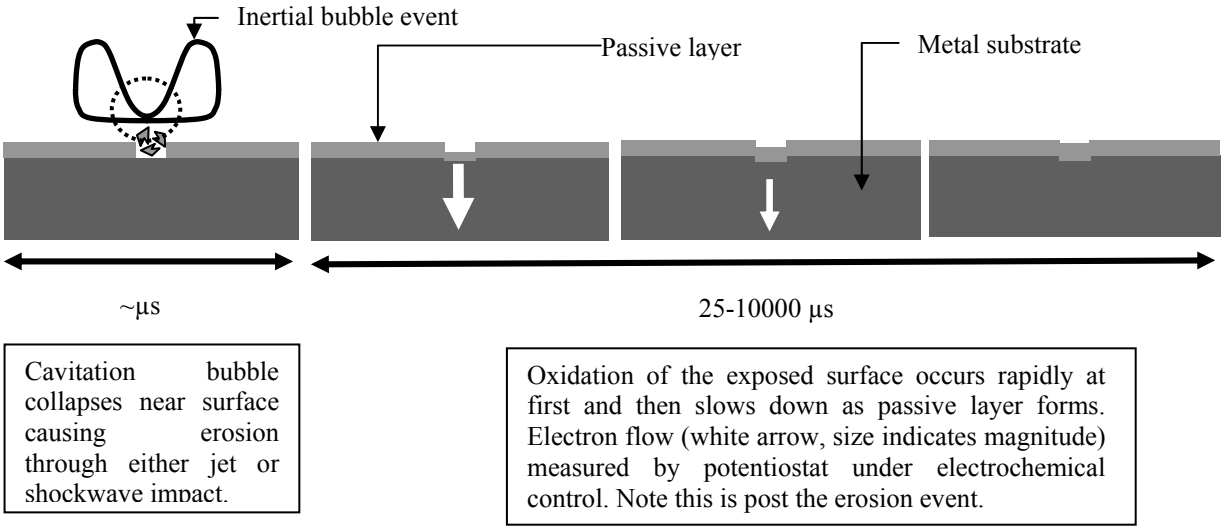

Fig.1 Schematic showing the time sequence associated with the erosion event. Note the electrochemical signal is only observed after the surface layer is damaged by the cavitation bubble collapse

monitor the erosion of the interface as a function of time and space. For example if we consider a Pb system, under appropriate conditions of potential and solution composition, the surface of this electrode can be coated with an insoluble $PbSO_4$ layer. In the event of an erosive event (such as the collapse of an inertial cavitation bubble close to the solid/liquid interface), material is removed from the surface. The electrode is held under electrochemical control and hence the initial $PbSO_4$ surface reforms. The associated electrons are registered as an anodic current at the electrode surface. Figure 1 shows the sequence of events and the associated time periods. Note the electrochemical data is post the erosion event. However, the electrochemical current time transient registered is relatively fast depending on the system. For example an erosion event recorded at a $Pb/PbSO_4$ interface is of the order of 100 μs in duration while transients at passivated Al electrodes are < 50 μs in length [19].

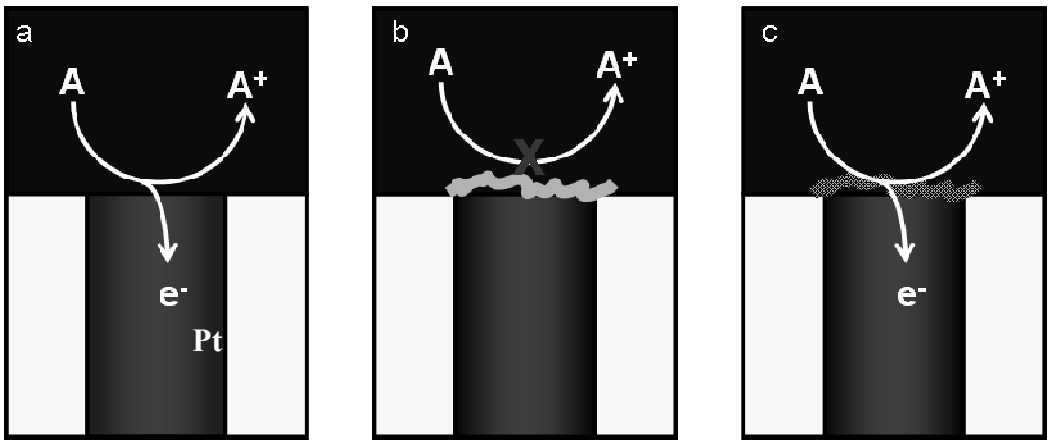

Fig.2 Schematic of surface cleaning using a redox probe (A) and a non-permeable matrix (■). Frame (a) denotes the electrochemical oxidation of 'A' at a clean Pt interface. Frame (b) represents the blocking of the interface by the non-permeable matrix while Frame (c) represents the result of cleaning the interface and the electrochemical oxidation of 'A' at the Pt interface

While this represents the erosion of the solid/liquid interface, it may not represent 'cleaning' of the interface. In many practical applications the removal of poorly soluble layers from the solid liquid interface is required. Here electrochemical measurements are also of use. If we consider a platinum electrode placed in a solution containing an appropriate redox species (for example $Fe(CN)_6^{3-}$), if the electrode surface is coated with a non permeable matrix, electrochemical oxidation or reduction of the redox system is note possible. However, if the surface is cleaned by an appropriate mechanism, the electrochemically active material is able to reach the surface of the electrode. Hence if the electrode is held at an appropriate potential, electrochemical oxidation or reduction of the redox species in the solution can now be invoked.

Clearly this represents a novel way to monitor the cleaning of the interface. Figure 2 shows a schematic representation of the proposed scheme. Figure 2 (a) shows how the bare electrode is able to electrochemically oxidize (under mass transfer limited conditions) 'A' at the interface. However, if the interface is blocked by a non permeable matrix, this signal is lost (see Figure 2 (b).) Finally, if an appropriate cleaning mechanism is employed, the removal of the non-permeable matrix is invoked and electrochemical accessibility is regained (see figure 2 (c)). The electrochemical detection of surface cleaning is an analytical approach to this problem, the results of which are discussed in the following sections. Lastly it must be noted that in order to understand the results obtained from this study, an appreciation of the sound field generated by the particular sound source employed is vital.

In this study, a piston like emitter is used as an appropriate sound source operating at ~ 23 kHz. Full description of this source and its characteristics can be found elsewhere [4]. In brief the direct sound field produced by this source decays in amplitude relatively quickly from the source so that pressure amplitudes in the 10's of kPa are encountered at distances > 3 mm [4]. However, due to the nature of the cavitation environment, and the generation of a cluster collapse [14, 20, 21] system, the sound field also possesses higher frequency components associated with the shock like emission from the cluster. This complicates the sound field as both the direct field and the bubble field are of importance. Indeed the presence of the high frequency components of the system results in the interaction of the sound field with relatively small objects (for example a 2 mm diameter glass electrode body). Hence care must be taken as insertion of items into the field can result with interactions with this complex sound field [22]. In addition to these complications, an accurate control of the distance between the emitting surface of the piston like emitter and the electrode is required. Nevertheless careful experimental design, consideration of the sound field and the associated bubble processes can enable valid conclusions to be drawn from these often complex environments, particularly if a multi-sensor approach is employed. The results of such a strategy applied to surface cleaning are now presented.

1. EXPERIMENTAL

All electrochemical cleaning experiments were carried using the setup shown in Figure 3. A cylindrical glass cell (75 mm internal diameter × 105 mm height) was used, which was fitted with a flat window to allow high-speed imaging. The cell also had an SQ 13 joint fitted to the base, which allowed electrodes to be inserted and sealed with a silicone washer. The cell was placed on a fixed stand and the ultrasonic horn entered the top of the cell such that the surface of the tip was parallel with the surface of the electrode (the so-called 'face-on' arrangement). The transducer itself was fixed to a computer controlled XYZ rig (3× Zaber T-LA60 linear actuators and stages). This allowed the position of the horn to be moved 60 mm in each

direction with a resolution of greater than 10 μm. The cell was filled with 250 cm^3 of aerobic solution (20-25 ^oC).

Ultrasound and cavitation were generated by means of a Grundig Digimess FG 100 function generator, Brüel & Kjær Type 2713 power amplifier and ultrasonic transducer fitted with a 3 mm diameter titanium tip (Adaptive Biosystems) [23]. The function generator was interfaced with a PC using software written in-house, allowing the frequency, power and duration of the ultrasound to be accurately controlled. The nominal frequency of the ultrasound was ~23 kHz.

High-speed imaging data was recorded using a Photron APX 250RS digital camera fitted with a Navitar 12× zoom lens. The subject was backlit using a Schott DCR III cold light source with the fibre optic removed (*i.e.* the light from the lamp was used directly). This set up resulted in the subject being in silhouette. The camera was triggered using a TTL pulse generated by a National Instruments PCI-6025E ADC card. In cases where high-speed imaging and electrochemical data were recorded synchronously the same pulse was used to trigger the camera and the electrochemical data acquisition.

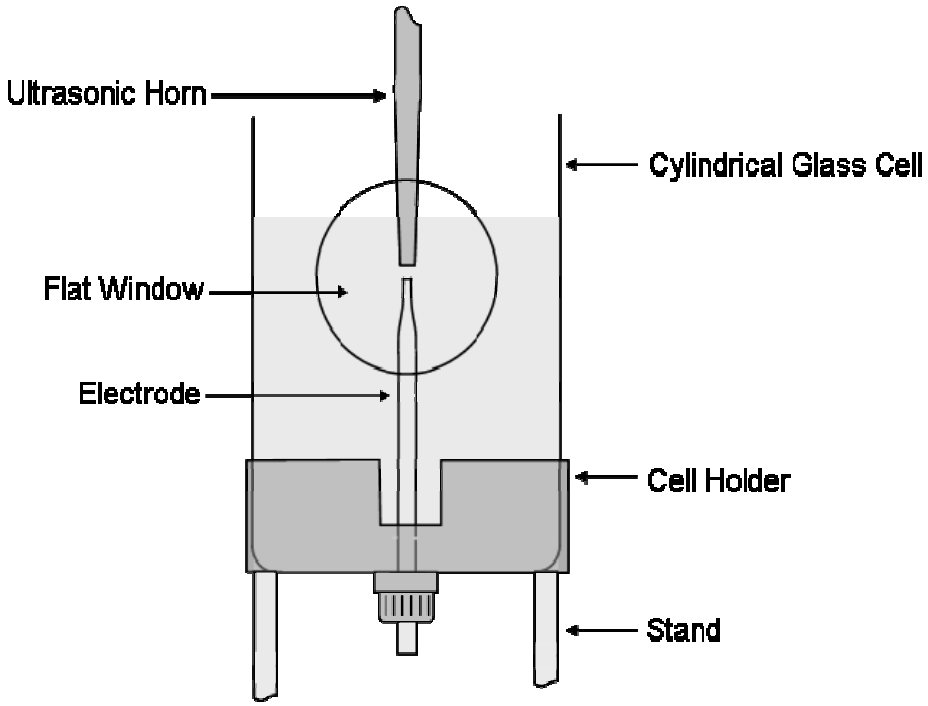

Fig.3 Schematic view of the electrochemical cleaning experimental setup

For erosion detection experiments a two electrode setup was used with a silver wire acting as a reference/counter electrode. A custom built current follower with an additional optocoupled logic gate output was used. The logic gate was such that when the current output was low the logic output was high (5 V) and when the current output was high, the logic output was low (0 V). The low/high threshold in the current could be controlled using a variable resistor attached to the chip. This system means that it is possible to record the current as a function of time and also use the counter feature on the ADC card (which responds to TTL pulses) to count peaks easily. This was used in the investigation of the erosion threshold.

For decontamination experiments, electrochemical data was acquired using a three electrode system with a Pt mesh acting as the counter electrode and a saturated calomel electrode (SCE) as the reference. The potential of the working electrode was controlled using

a potentiostat built in-house and the current was recorded using a PC, ADC card (National Instruments PCI-6025E) and software developed in-house.

Platinum electrodes (0.5 mm diameter) and stainless steel electrodes (25 μm diameter) were prepared by sealing the appropriate wire in glass (work undertaken by the Scientific Glassblowers at the University of Southampton). The surfaces of the electrodes were polished flat using silicon carbide paper (up to 1200 grade) and in the case of the stainless steel electrodes the faces were further polished with aqueous alumina slurries (1 μm). Recessed platinum electrodes were prepared by etching the metal using a two-electrode arrangement with a vitreous carbon rod acting as the counter electrode. The applied potential was switched between +6 V and –6 V at a frequency of 25 Hz (0.02 second pulses). The etching solution consisted of 60% saturated $CaCl_2$, 36% H_2O and 4% concentrated HCl (by volume). During etching, the solution was cavitated at a distance of 5 mm in order to remove reaction products from the cavity, which were found hinder the etching process if not removed. The progress of the etching was monitored using the high-speed camera (in live mode to act as a microscope). Following the etching process the electrode was thoroughly rinsed with distilled water. In all experiments the foulant used was thickened methyl salicylate (tMS). In the case of the flat surfaces and the 0.5 mm diameter recessed electrodes, tMS was applied (either on to the flat surface or into the recess) using a 34G MicroFil needle. The amount was not controlled but was in the region of 0.02 g.

The pump system used to assess the effects of bulk fluid flow alone is shown in Figure 4. The pump (Eheim Type 1105) was fitted with a 10 mm inlet and the outlet nozzle was a pipette tip, cut so that the outlet was 3 mm diameter (the same as the ultrasonic horn). The pump was rated at 4.5 l min^{-1}. For pump experiments the nozzle assembly was fitted to the XYZ stage in place of the transducer and horn.

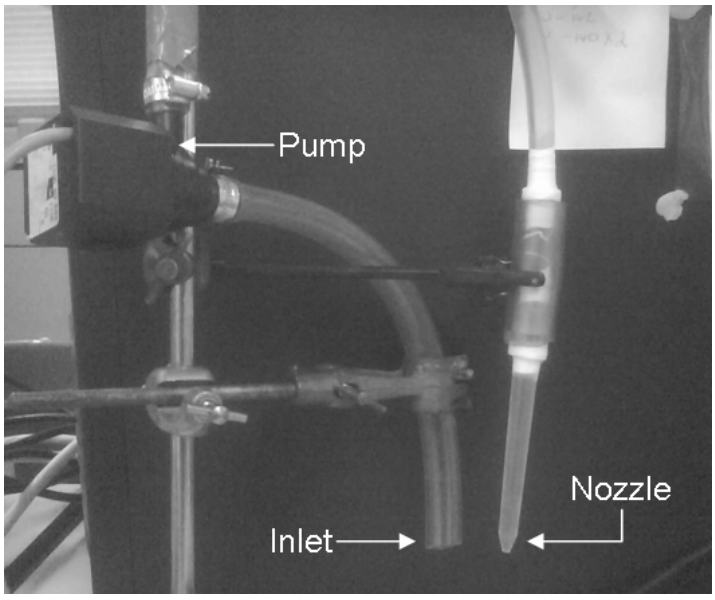

Fig.4 Pump system used to assess the effects of bulk fluid flow

All solutions were made up using water from either a USF Elga Purelab Option 10 or Purite Select water purification system. Water purified in this manner had a conductivity below 0.06 μS cm^{-1}. All chemicals, which were used as supplied, are shown in Table 1.

Tab.1 List of chemicals, suppliers and purity used in this work

Chemical	Supplier	Purity
Methyl salicylate (thickened)	DSTL	-
Potassium ferricyanide	Aldrich	99+ %
Sodium sulphate	Fisher Scientific	Laboratory reagent grade
Strontium nitrate	Aldrich	99+ %

2. RESULTS AND DISCUSSION

In order to access the extent of surface erosion as a function of distance, a passivated stainless steel electrode, held under potential control, can be used as sensor to detect cavitation induced erosion/corrosion. Figure 5 shows a typical current-time trace for such an approach with the electrode held at +0.9 V *vs.* Ag in a solution of 0.1 M Na_2SO_4.

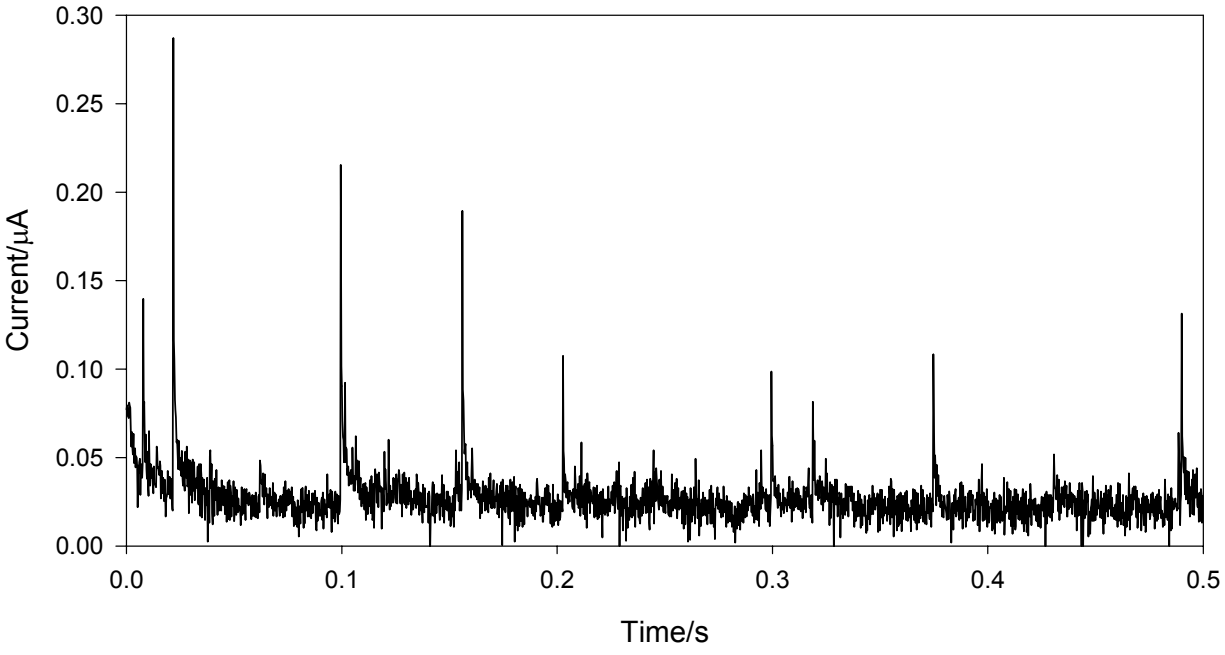

Fig.5 Plot showing the current measured as a function of time at a 25 μm diameter stainless steel electrode exposed to ultrasound in a solution of 0.1 M Na_2SO_4. The electrode was held at a potential of +0.9 V *vs.* Ag. The distance between the tip of the sound source and the electrode was 0.5 mm

Under these conditions the electrode was passivated by a layer of insoluble oxide. The erosion of this layer [15, 16] (or parts of it) leads to spontaneous re-passivation of the exposed metal. This results in transient current spikes, a number of which can be seen in Figure 5. At times outside the occurrences of these transients the surface of the electrode remains passivated and little current flows. Having determined that cavitation-induced erosion/corrosion does occur within the system, the extent of the erosion as a function of axial

distance was measured. In order to measure the maximum distance at which erosion/corrosion events are detected a number of approaches towards the sound source were employed. Here the electrode was positioned at greater distances (e.g. > 3 mm) from the sound source and then moved towards the sound source until an event was registered. This process was repeated until an accurate measure of the erosion/corrosion limit was found for the stainless steel electrode employed. Note this method ensures that erosion damage to the surface of the electrode is kept to a minimum. The results obtained from this experiment (20 consecutive approaches towards the sound source) indicate an average threshold distance for the detection of inertial events (as defined by erosion of the passive layer) of 870 ± 25 μm. However, this distance will be dependant on the mechanical nature of the passive film. If a softer material is employed (e.g. a salt such as $PbSO_4$) the erosion limit extends to 1.5 - 2.5 mm and will also depend on the electrode construction [4]. Nevertheless, these experiments have shown that erosion of the surface only occurs close to the source. However, surface cleaning in the form of degreasing is of importance as this is relevant to the cleaning of sensitive objects which may not withstand the harsh conditions required to remove oxide from the surface. Hence another set of experiments were performed relying on the removal of an organic layer from a Pt surface.

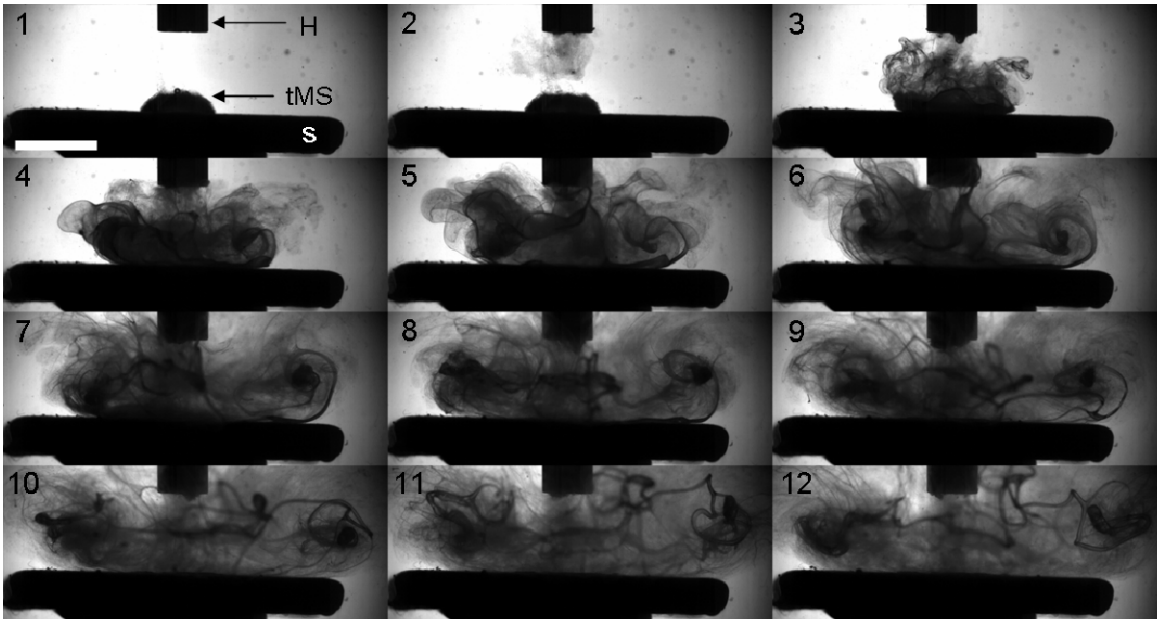

Fig.6 Image showing 12 frames taken from high-speed imaging data show a dummy sample contaminated with tMS exposed to ultrasound. The distance between the sound source and the sample was 5 mm. The sample is labelled 's' in frame 1 and the horn is labelled 'H'. The time between frames was 0.02 s and the exposure time was 1/150000 s. The scale bar represents 5 mm

Figure 6 shows a set of images obtained from a high-speed camera following the removal of a drop of an insoluble organic material (thickened methyl salicylate, tMS) from a surface. In this experiment the sound source was position at a distance of 5 mm from a solid support

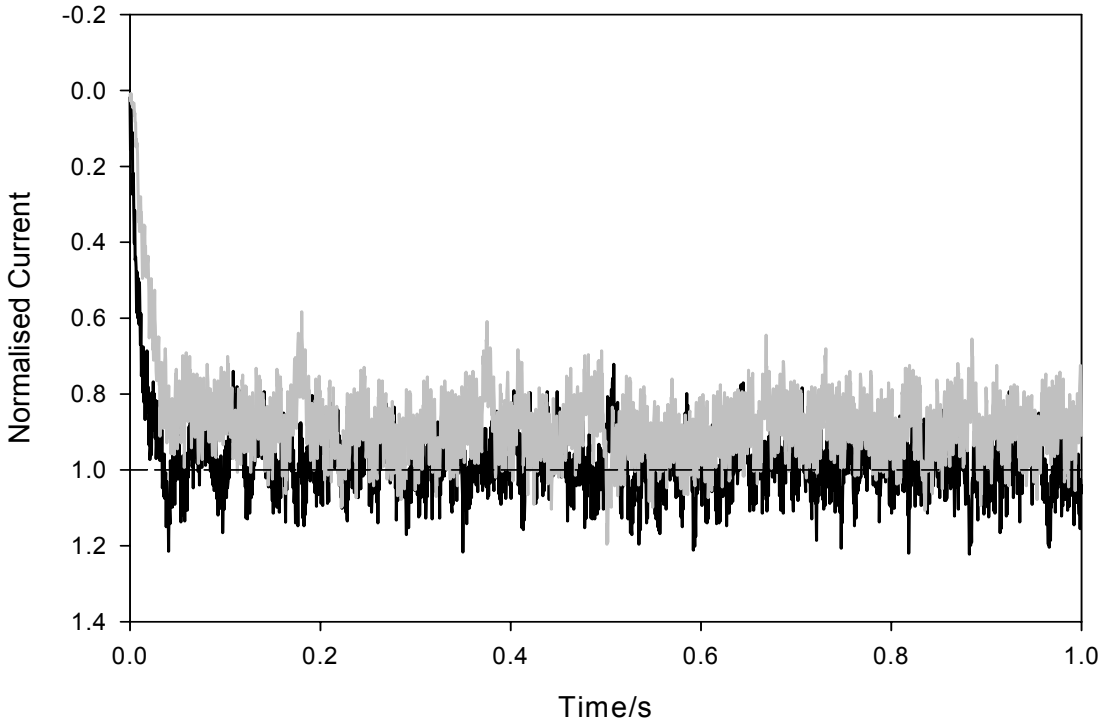

Fig.7 Plot showing the current recorded at a tMS coated (—) and clean (—) 0.5 mm diameter Pt electrode in 5 mM $K_3Fe(CN)_6$ and 0.1 M $Sr(NO_3)_2$ as a function of time. Ultrasound was turned on at t = 0 s. The distance between the horn and electrode was 5 mm. The potential of the electrode was held at 0 V *vs.* SCE

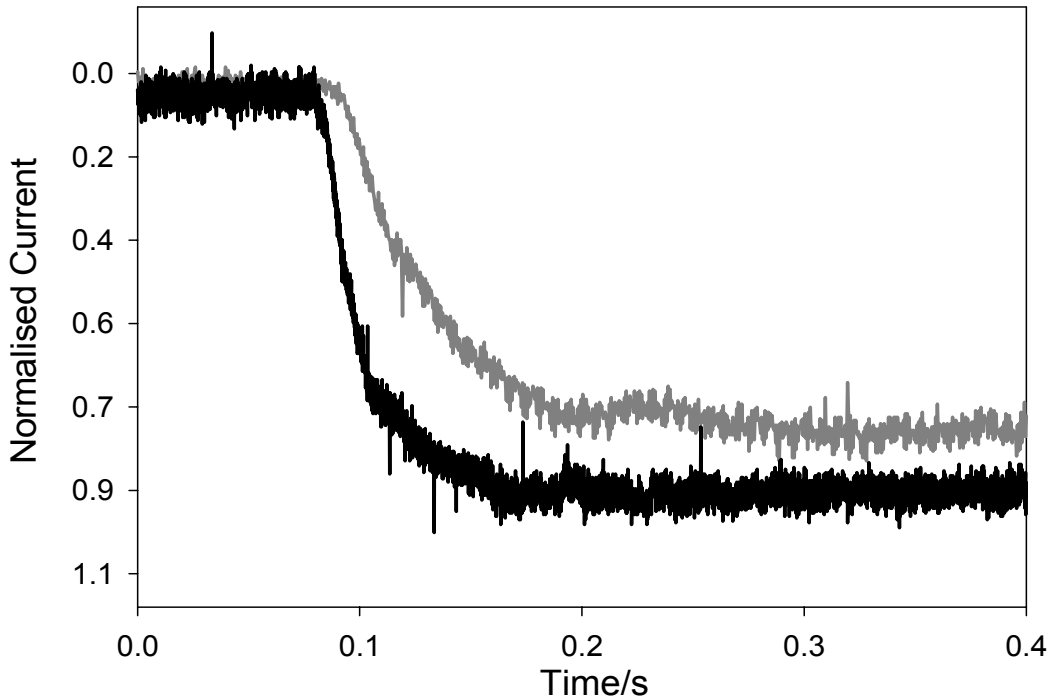

Fig.8 Plot showing the current recorded at a coated (—) and clean (—) 0.5 mm diameter Pt electrode in an emulsion solution with 5 mM $K_3Fe(CN)_6$ and 0.1 M $Sr(NO_3)_2$ as a function of time. Pump was turned on at t = 0 s. The distance between the horn and nozzle was 5 mm. The potential of the electrode was held at 0 V *vs.* SCE

(labelled ‘s’). In frame 1 the ultrasound was off and it was initiated between frames 1 and 2. Over the next 9 frames the tMS is removed from the surface and broken up into small string-like fragments, which can be seen particularly clearly on frames 10-12. Note this experiment was performed outside the inertial zone (see above) and indicates that cleaning from the solid/liquid interface in this case does not solely require this phenomenon. In order to gather more analytical information relating to the rate at which material is removed from the surface under these conditions, a set of experiments investigating the blocking of a surface with tMS was initiated. Here the degree of surface cleaning was measured by following the Faradaic current recorded at a Pt electrode held at the mass transfer limiting potential of $Fe(CN)_6^{3-}$ in aqueous solution. At the start of each experiment a drop of tMS was applied to the electrode and the current monitored as a function of time. Cleaning of the interface resulted in an increase in the Faradaic current. In order to quantify the degree of cleaning, the current was normalised to that in the absence of any foulant but the presence of power ultrasound. Hence‘1’ represents a clean interface will ‘0’ a blocked interface. Figure 7 indicates that under these conditions the removal of the tMS droplet occurs relatively quickly (< 0.1 s). Indeed the current increase at the bare Pt electrode surface (due to forced convection of material to the electrode) rings up over approximately the same time period as that found for the coated electrode. This implies that removal of the tMS is relatively efficient at this extended distance and considering the preceding erosion limit (< 3 mm for this system) indicates that inertial cavitation is probably not directly involved. However, solution flow induced by the sound field and bubble dynamics is known to be present in these systems. Note figure 6 shows that the tMS is washed from the surface by the action of the ultrasonic source. Hence quantification of this flow was required. Using high speed camera experiments (not shown), the flow rate at a distance of 5 mm generated by the horn was found to be 2450 ± 370 mm s^{-1}.

In order to test the effect of this flow on surface cleaning a simple pumped jet system was developed (see figure 4). This system was capable of generating a flow velocity of 3620 ± 230 mm s^{-1}. Figure 8 shows a comparison between a tMS coated electrode and a clean electrode of the current time transients obtained as the pump system was initiated. Although some variation was observed, the pump turn on delay (~ 0.1 s) suggests that the surface cleaning as a result of the flow of the pump is comparable to those cleaning times produced by the ultrasonic horn.

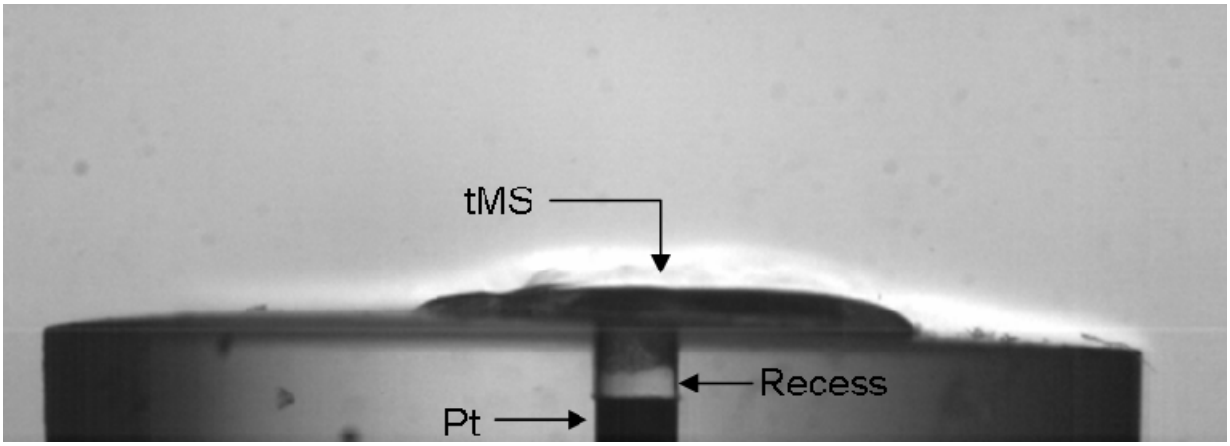

Fig.9 Example of a recessed electrode contaminated with tMS. The Pt wire is 0.5 mm in diameter and the recess was ~0.4 mm

These results imply that the cleaning effect on these electrode substrates are likely to be associated with the flow of liquid from the tip of the ultrasonic horn (created by acoustic streaming etc. [24, 25]). Clearly in order to assess the effectiveness of ultrasound on the removal of material from a surface, further more stringent experiments are required. In this case a recessed electrode was developed and filled with tMS (see figure 9). The cleaning of this electrode was then assessed in the presence of ultrasound or pump induced flow. Figure 10 shows the effect of the recess on pump flow cleaning of the Pt surface. This shows that the presence of the recesses severely limits cleaning of the surface. Indeed, even when the time window of the experiment was extended to 1000 s the recess could not be fully cleaned out.

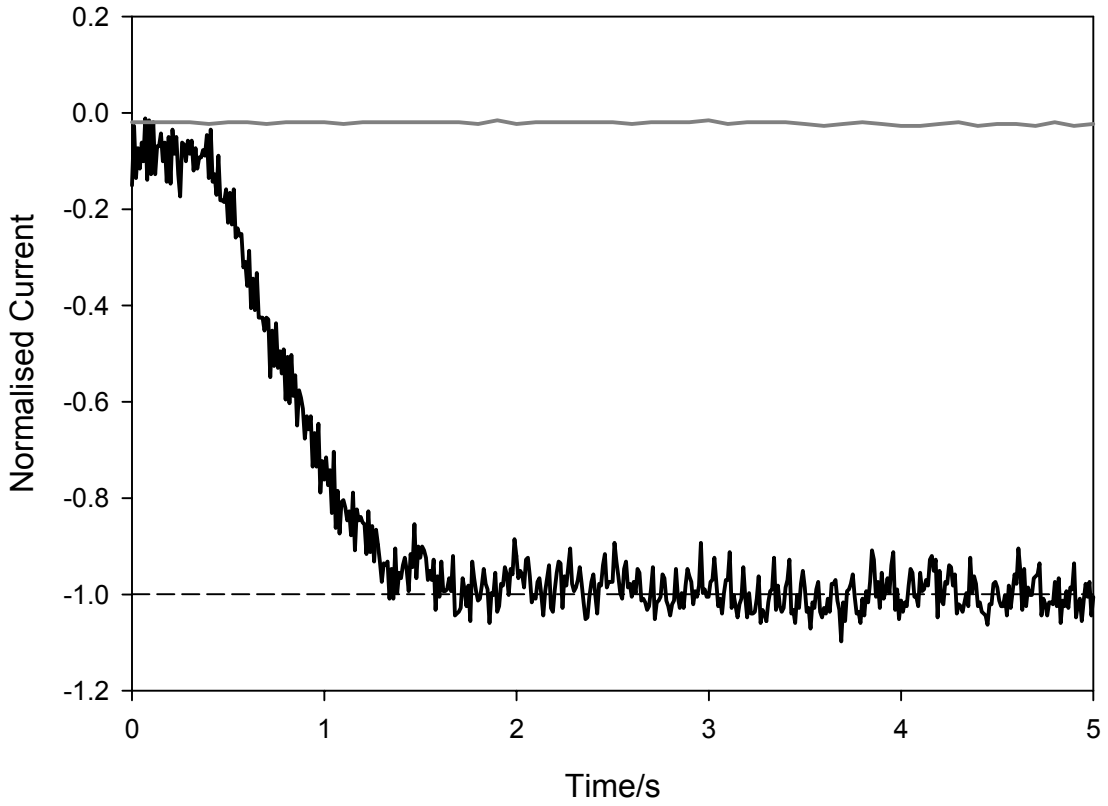

Fig.10 Plot showing the current measured as a function of time at a coated (—) and uncoated (▬) recessed Pt electrode (0.5 mm diameter × 0.4 mm depth) exposed to bulk fluid flow generated by a pump in an solution containing 5 mM $K_3Fe(CN)_6$ and 0.1 M $Sr(NO_3)_2$. The distance between the horn and nozzle was 5 mm. The potential of the electrode was held at 0 V *vs.* SCE

This implies that flow alone is unable to remove this material from the electrode surface. In comparison the ability of ultrasound to remove the tMS from the electrode assembly was significantly better. Figure 11 shows that under similar conditions ultrasonic irradiation of the system is able to remove the tMS in around 0.14 s after initiation of the ultrasonic source. Clearly this represents a significant advantage compared to flow alone (see figure 10). Further high-speed imaging experiments (not shown) indicate that the mechanism responsible for this enhancement is bubble related. This effect is currently under further investigation.

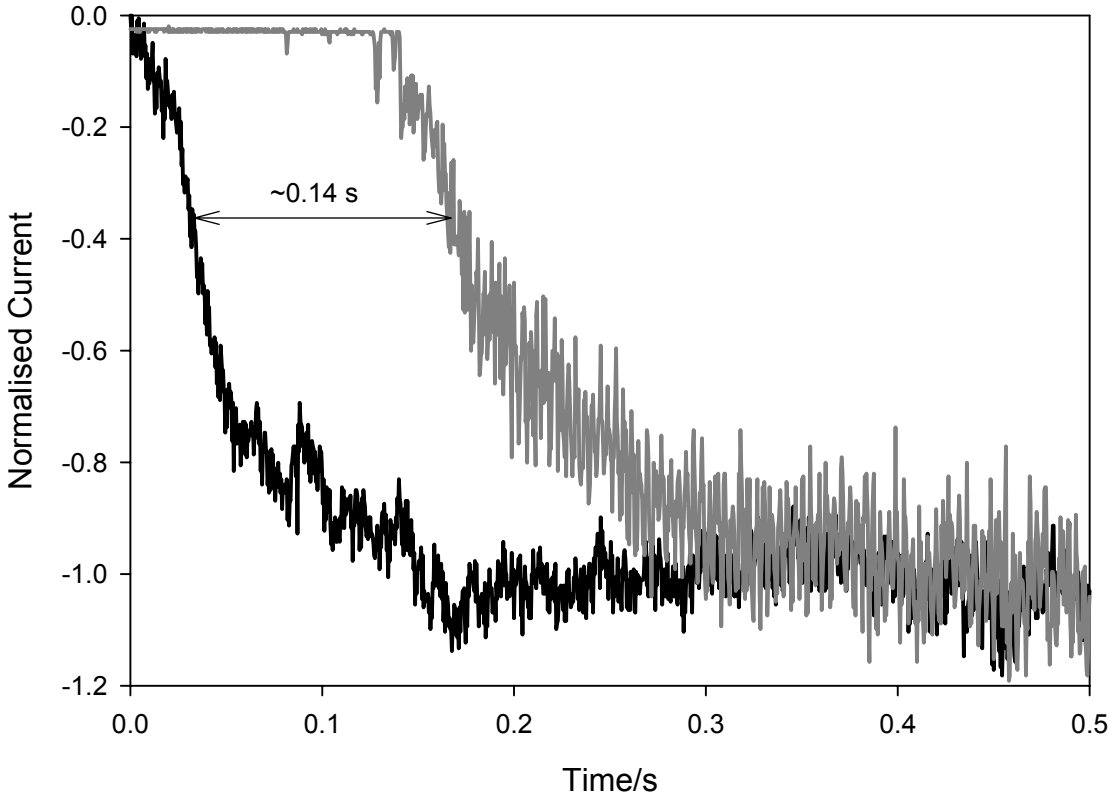

Fig.11 Plot showing the current recorded at a coated (—) and clean (▬) 0.5 mm Pt electrode in an emulsion solution with 5 mM $K_3Fe(CN)_6$ and 0.1 M $Sr(NO_3)_2$ as a function of time. Ultrasonic irradiation was initiated at $t = 0$ s. The distance between the source and electrode was 5 mm. The potential of the electrode was held at 0 V *vs.* SCE

3. CONCLUSIONS

The erosion/corrosion measurements performed with a passivated 25 µm diameter stainless steel electrode indicate that inertial cavitation cleaning only works at short source to surface distance of ~ 900 µm. However, cleaning at extended distances (here 5 mm) was observed for an insoluble matrix placed on an electrode surface. For flat interfaces, flow from the sound source (or pump) was able to remove the test material employed. However, if the structure was recessed, ultrasound was significantly better at removing the insoluble matrix from the substrate.

ACKNOWLEDGEMENTS

The authors thank the EPSRC (grant No: EP/D05849X/1) and dstl for funding.

REFERENCES

1. L. E. Kinsler, A. R. Frey, A. B. Coppens and J. V. Sanders, Fundamentals of Acoustics, John Wiley & Sons, 1982 New York.

2. P. M. Morse and K. U. Ingard, Theoretical Acoustics, Princeton University Press, 1986 New York.
3. P. R. Birkin, T. G. Leighton, J. F. Power, M. D. Simpson, A. M. L. Vinçotte and P. F. Joseph, Experimental and Theoretical Characterisation of Sonochemical Cells. Part 1. Cylindrical Reactors and Their Use to Calculate the Speed of Sound in Aqueous Solutions., Journal of Physical Chemistry A, 107, 2003.
4. P. R. Birkin, D. G. Offin and T. G. Leighton, Experimental and theoretical characterisation of sonochemical cells - Part 2 Cell disruptors (Ultrasonic horns) and cavity cluster collapse, PCCP, 7, 2005.
5. T. G. Leighton, The Acoustic Bubble, Academic Press, 1994 London.
6. P. R. Birkin, T. G. Leighton and Y. E. Watson, Applications of Power Ultrasound in Physical and Chemical Processing 4, Besançon, 2003.
7. H. G. Flynn, Cvaitation Dynamics I. A mathematical formulation, Journal of the Acoustics Society of America, 57, 1975.
8. R. E. Apfel, Cavitation and Inhomogeneities in underwater acoustics, Gottingen, 1980.
9. R. E. Apfel, in *Methods in Experimental Physics*, ed. P. D. Edmonds, Academic Press, New York, 1981, vol. 19.
10. C. K. Holland and R. E. Apfel, An Improved Theory for the Prediction of Microcavitation Thresholds, IEEE Transactions Ultrasonics Ferroelectrics and Frequency Control, 36, 1989.
11. E. B. Flint and K. S. Suslick, The Temperature of Cavitation, Science, 253, 1991.
12. K. S. Suslick, D. A. Hammerton and R. E. Cline, The Sonochemical Hotspot, Journal of the American Chemical Society, 108, 1986.
13. P. R. Birkin, D. G. Offin and T. G. Leighton, Experimental and theoretical characterisation of sonochemical cells. Part 2: cell disruptors (Ultrasonic horns) and cavity cluster collapse, Phys. Chem. Chem. Phys., 7, 2005.
14. B. Vyas and C. M. Preece, Stress produced in a solid by cavitation, Journal of Applied Physics, 47, 1976.
15. G. O. H. Whillock and B. F. Harvey, Ultrasonically enhanced Corrosion of 304L Stainless Steel II: The effect of frequency, acoustic power and horn to specimen distance., Ultrasonics Sonochemistry, 4, 1997.
16. G. O. H. Whillock and B. F. Harvey, Ultrasonically enhanced corrosion of 304L stainless steel I: The effect of temperature and hydrostatic pressure., Ultrasonics Sonochemistry, 4, 1997.
17. P. R. Birkin, R. O'Connor, C. Rapple and S. Silva-Martinez, Electrochemical measurement of erosion from individual cavitation generated from continuous ultrasound, Journal of the Chemical Society Faraday Transactions, 94, 1998.
18. P. R. Birkin, D. G. Offin and T. G. Leighton, The study of surface processes under electrochemical control in the presence of inertial cavitation, Wear, 258, 2005.
19. C. J. B. Vian, A comparison of measurement techniques for acoustic cavitation, PhD, University of Southampton, 2007.
20. I. Hansson, V. Kedrinskii and K. A. Morch, On the dynamics of cavity clusters, Journal of Physics D: Applied Physics, 15, 1982.
21. I. Hansson and K. A. Morch, The dynamics of cavity clusters in ultrasonic (vibratory) cavitation erosion, Journal of Applied Physics, 51, 1980.
22. P. R. Birkin, D. G. Offin, P. F. Joseph and T. G. Leighton, Cavitation, shock waves and the invasive nature of sonoelectrochemistry, Journal Of Physical Chemistry B, 109, 2005.
23. D. G. Offin, An investigation of fast surface re-formation in the presence of inertial (transient) cavitation, PhD, University of Southampton, 2006.

24. F. Marken, J. C. Eklund and R. G. Compton, Voltammetry in the presence of ultrasound, Journal of Electroanalytical Chemistry, 395, 1995.
25. H. H. Zhang and L. A. Coury, Effects of High-Intensity Ultrasound on Glassy-Carbon Electrodes, Analytical Chemistry, 65, 1993.